Hindawi Publishing Corporation
EURASIP Journal on Wireless Communications and Networking
Volume 2011, Article ID 670637, 12 pages
doi:10.1155/2011/670637

Research Article

Bit Error Rate Analysis for an OFDM System with Channel Estimation in a Nonlinear and Frequency-Selective Fading Channel

Amir Ligata,[1] Haris Gacanin,[2,3] Fumiyuki Adachi,[4] Miha Smolnikar,[5] and Mihael Mohorcic[5]

[1] *IPSA Institute, 71000 Sarajevo, Bosnia and Herzegovina*
[2] *Alcatel-Lucent Bell N.V., 2018 Antwerpen, Belgium*
[3] *Communication Group at Energy and Communication Department, IPSA Institute, 71000 Sarajevo, Bosnia and Herzegovina*
[4] *Department of Electrical and Communication Engineering, Graduate School of Engineering, Tohoku University, Sendai 980-8579, Japan*
[5] *Jozef Stefan Institute, 1000 Ljubljana, Slovenia*

Correspondence should be addressed to Amir Ligata, amir.ligata@ipsa-institut.com

Received 27 December 2010; Accepted 21 February 2011

Academic Editor: Ibrahim Develi

Orthogonal frequency division multiplexing (OFDM) is an effective technique for high-speed digital transmission over time-dispersive channels. However, for coherent detection, a reliable channel estimation (CE) is required. OFDM is characterized by its high peak-to-average power ratio (PAPR), which makes it very sensitive to nonlinear distortions that may affect the channel estimation accuracy leading to a bit error rate (BER) performance degradation. In this paper, we present closed-form BER expression for OFDM with a pilot-assisted CE in a nonlinear and frequency-selective fading channel. We discuss how, and to what extent, the nonlinear degradation affects the BER performance with the CE based on a time/frequency division-multiplexed (TDM/FDM) pilot. The analysis is based on a Gaussian approximation of the nonlinear noise due to both HPA amplitude limitation and quantization. We also evaluate the estimator's mean square error (MSE) with both TDM and FDM pilots. Our results show that pilot-assisted CE using FDM pilot is more sensitive to nonlinear distortions than the CE using a TDM pilot, since its pilot subcarriers are affected by nonlinear noise due to both the HPA and the quantization.

1. Introduction

In a terrestrial radio channel, the transmitted signal reaches the receiver through multiple propagation paths, which all have a different relative delay and gain. This produces inter-symbol interference (ISI) and degrades the system's performance [1]. Orthogonal frequency division multiplexing (OFDM) can be used to overcome the channel frequency selectivity, but it requires an accurate channel estimation (CE) for coherent detection. Various CE schemes have been proposed for OFDM [2–5], where the pilot signals are multiplexed either in the time (TDM pilot) or in the frequency domain (FDM pilot). In a fading channel, the performance of an OFDM system with CE using a TDM pilot gets rapidly degraded whenever the channel has a significant time variance. On the other hand, the CE with an FDM pilot improves the tracking against a fast fading, but the performance degrades, since the noise is spread over all subcarriers due to interpolation.

The main drawback of OFDM is its high peak-to-average power ratio (PAPR), which makes the system very sensitive to nonlinear distortions caused by analog components, such as a high-power amplifier (HPA) as well as digital-to-analog (DA) and analog-to-digital (AD) converters. Usually, DA and AD converters are assumed to have a large number of quantization levels and an optimally exploited dynamic range. Because of such assumptions, the quantization noise (representing the quantizer granularity) and the noise due

to amplitude limitation (corresponding to the overloading distortion) can be neglected [6–8]. However, in a real implementation, in order to keep the system complexity and the power consumption low, it is desirable to keep the resolution of the DA/AD converters as low as possible [9, 10]. It was shown, in [11], that the quantization requirements are higher at the receiver end, particularly for severely frequency-selective channels. The analysis of the nonlinear distortions due to amplitude clipping in an OFDMA system is presented in [12], where it was shown that users with less allocated power are subject to stronger nonlinear interference. In [13], the impact of the nonlinear degradation due to amplitude clipping on an OFDM system's transmission performance was investigated with a computer simulation. To the best of the authors' knowledge, closed-form BER expressions for an OFDM system with CE in a nonlinear and frequency-selective fading channel has not been presented.

In this paper, we present a theoretical analysis of an OFDM system with a pilot-assisted CE based on TDM and FDM pilots in a nonlinear and frequency-selective fading channel. We derive a closed-form BER and mean square error (MSE) expressions and discuss the sensitivity of both CE schemes to the nonlinear and channel impairments. Unlike previous papers, where nonlinear noise due to the HPA and the quantization is treated separately, we take into consideration the effects of both. Our analysis is based on a Gaussian approximation of the nonlinearity due to the HPA amplitude saturation and the insufficient resolution of the quantization. The results show that the BER performance with pilot-assisted CE based on an FDM pilot is more sensitive to the nonlinear distortion then a TDM pilot, since its pilot subcarriers are affected by nonlinear noise due to both the HPA and the quantization.

The rest of the paper is organized as follows. Section 2 gives an overview of the system model. A performance analysis is given in Section 3, while the numerical results and discussions are presented in Section 4. The conclusion of the paper is set out in Section 5.

2. System Model

The OFDM transmission system model is illustrated in Figure 1. Throughout this paper, T_c-spaced discrete time representation is used, where T_c represents the fast Fourier transform (FFT) sampling period. The mathematical signal representation and brief overview of pilot-assisted CE schemes are presented next.

2.1. Mathematical Signal Representation. The mth ($m = \ldots, -1, 0, 1, \ldots$) frame of the N_c data-modulated symbols $\{d_m(k);\ k = 0 \sim N_c - 1\}$ with $E[|d_m(k)|^2] = 1$ is transmitted during one $T_s = N_c T_c$ signaling interval. The data-modulated symbol sequence $\{d_m(k)\}$ is fed to an N_c-point inverse FFT (IFFT) to obtain the time-domain OFDM signal $\{s_m(t);\ t = 0 \sim N_c - 1\}$.

The nonlinear noise is introduced to the system through an DA conversion and a HPA, as depicted in Figure 2. The OFDM signal is fed to a DA converter to transform

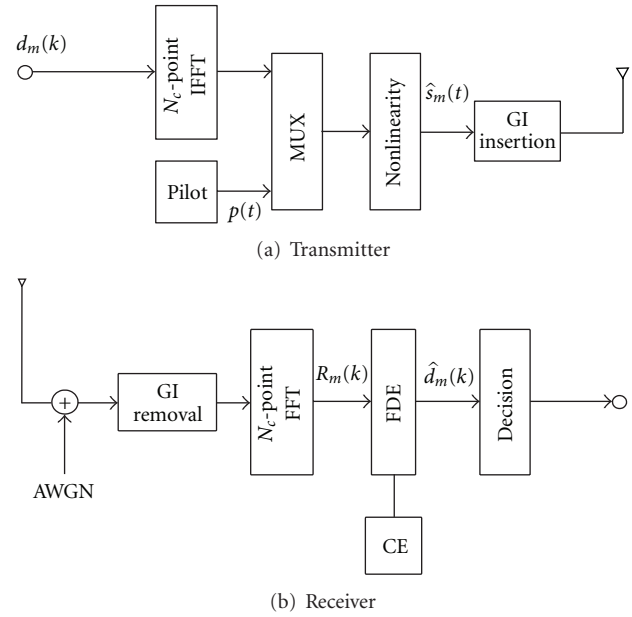

Figure 1: OFDM system model.

the signal from the digital to the analog domain. The DA conversion is represented by the quantization model given in [7]. For quantization with R-bit resolution (i.e., $M = 2^R$ quantization levels), the signal after the quantization is expressed as $s_m^{\mathrm{DA}}(t) = \{s_m^{\mathrm{DA}}(t)\}^I + j\{s_m^{\mathrm{DA}}(t)\}^Q$. The in-phase ($I$) and quadrature ($Q$) signal components are given as $\{s_m^{\mathrm{DA}}(t)\}^I = q[\mathrm{Re}\{s_m(t)\}]$ and $\{s_m^{\mathrm{DA}}(t)\}^Q = q[\mathrm{Im}\{s_m(t)\}]$ with the quantization function defined as

$$s_m^{\mathrm{DA}}[|s_m(t)|] = \begin{cases} Q_{\mathrm{out}}, & |s_m(t)| > Q_{\mathrm{in}}, \\ \dfrac{Q_{\mathrm{out}}}{Q_{\mathrm{in}}}\left(\left\lfloor \dfrac{|s_m(t)|}{\Delta} \right\rfloor \Delta + \dfrac{\Delta}{2}\right) & -Q_{\mathrm{in}} \le |s_m(t)| \le Q_{\mathrm{in}}, \\ -Q_{\mathrm{out}}, & |s_m(t)| < -Q_{\mathrm{in}}, \end{cases} \tag{1}$$

where the $\lfloor \cdot \rfloor$ represents the floor function (i.e., rounding to the largest integer not greater than the argument) and the quantization step size is given by $\Delta = Q_{\mathrm{in}}(2/2^R - 1)$, where Q_{in} and Q_{out} denote the quantizer input and output signal amplitudes, respectively. The required quantization levels N_{DA} per dimension can be derived as $N_{\mathrm{DA}} = 2\lceil C/\Delta \rceil$, with $C = 3\sqrt{1 + \sigma_n^2}$, where σ_n^2 represents the variance of the additive white Gaussian noise (AWGN) [7] and $\lceil . \rceil$ denotes the ceiling function (i.e., rounding to the smallest integer not less than the argument). We assume that the DA converter may exceed the HPA amplitude saturation level as depicted in Figure 3.

The analog signal $\{s_m^{\mathrm{DA}}(t);\ t = 0 \sim N_c - 1\}$ is fed to the HPA, most oftenrepresented through its input-output

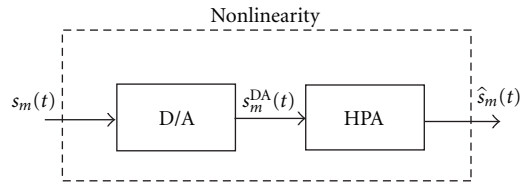

Figure 2: Nonlinearity model.

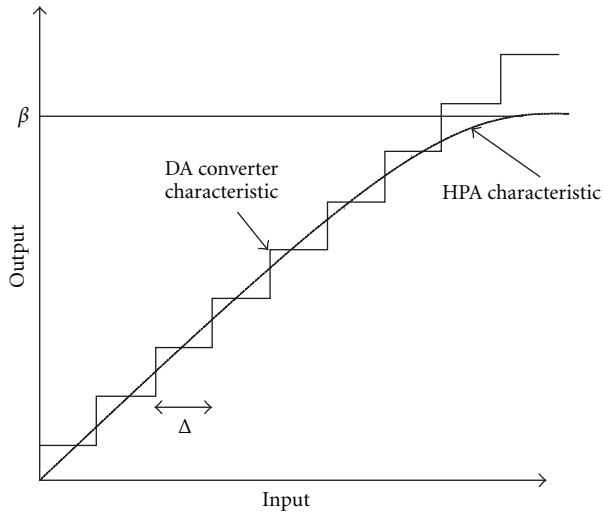

Figure 3: DA converter and HPA input-output characteristics.

characteristic [14], which may be approximated as

$$\hat{s}_m(t) = \begin{cases} s_m^{DA}(t), & |s_m^{DA}(t)| < \beta, \\ \beta \dfrac{s_m^{DA}(t)}{|s_m^{DA}(t)|}, & \text{otherwise}, \end{cases} \tag{2}$$

for $t = 0 \sim N_c - 1$, where β denotes the HPA amplitude saturation level. We note that the relation between β and the input backoff IBO is given as IBO $= 10\log_{10}(\beta^2/P_i)$, where P_i denotes the average input power. We emphasize that we introduce the clipping effect through an HPA, for which the input-output soft-limiter characteristic is approximated by (2). Thus, in this paper we refer to amplitude clipping as the amplitude saturation of the HPA. We also note that the PAPR at the output of the HPA is affected by β, irrespective of the CE scheme; a lower β will give a lower PAPR and vice versa [15].

An N_g-sample guard interval (GI) is inserted at the beginning of each OFDM frame, and the signal is multiplied by the power coefficient $\sqrt{2E_s/T_c}$, where E_s denotes the data-modulated symbol energy.

Using the Bussgang theorem [16], a nonlinear output can be expressed as the sum of the useful attenuated input replica and an uncorrelated nonlinear distortion as [16]

$$\hat{s}_m(t) = \sqrt{\frac{2E_s}{T_c N_c}}[\alpha s_m(t) + \tilde{s}_m(t)], \tag{3}$$

where α and $\tilde{s}_m(t)$, respectively, denote the attenuation constant and noise due to the nonlinearity. The attenuation constant α is chosen so as to minimize the MSE $E[|\hat{s}_m(t) - \alpha s_m(t)|^2]$ [17]. It is shown in [17] that for the amplitude saturation level $\beta > 7$ dB, $\alpha \to 1$. For lower β, α can be well approximated as $\alpha = 1 - \exp(-\beta^2) + (\sqrt{\pi}/2)\,\text{erfc}\{\beta\}$ [18], where erfc$\{\cdot\}$ denotes the complementary error function. The nonlinear noise after quantization and HPA can be expressed as $\tilde{s}_m(t) = \lambda_m(t) + \phi_m(t)$ for $t = 0 \sim N_c - 1$, where $\lambda_m(t)$ and $\phi_m(t)$, respectively, denote the noise due to HPA amplitude saturation, and the quantization. We assume that $\lambda_m(t)$ is approximated as a zero-mean random variable with the variance $2\sigma_c^2 = E[\lambda_m(t)\lambda_m^*(t)] = 1/N_c(1-\exp(-\beta^2)-\alpha^2)$ [17]. Furthermore, we assume that the quantization noise $\phi_m(t)$ is a zero-mean random variable with the variance σ_q^2 given by $E[\phi_m(t)\phi_m^*(t)] = \Delta^2/6$ [7], where Δ denotes the quantization step as illustrated in Figure 3.

After removing the GI, the received signal is decomposed into N_c-subcarrier components $\{R_m(k);\ k = 0 \sim N_c - 1\}$ given by

$$R_m(k) = \sqrt{\frac{2E_s}{T_c N_c}}[\alpha d_m(k) + \Lambda_m(k) + \Phi_m(k)]H_m(k) + \prod_m(k), \tag{4}$$

where $H_m(k)$, $\Lambda_m(k)$, $\Phi_m(k)$, and $\prod_m(k)$, respectively, denote the Fourier transforms of the mth frame's propagation channel gain, the distorted part of the output signal due to HPA saturation and the quantization and the additive zero-mean white Gaussian noise (AWGN) process with variance $2N_0/T_c$, where N_0 denotes the single-sided power spectrum density. To compensate for the channel distortion on each subcarrier, one tap frequency domain equalization (FDE) is applied as $\hat{d}_m(k) = R_m(k)w_m(k)$, where $w_m(k) = H_m^*(k)$ denotes the equalization weight [19]. Using (4), the equalized signal can be represented by

$$\hat{d}_m(k) = \sqrt{\frac{2E_s}{T_c N_c}}\left[\alpha d_m(k) + \Lambda_m(k) + \Phi_m(k)\right]\hat{H}_m(k) + \widehat{\prod_m}(k), \tag{5}$$

with

$$\begin{aligned} \hat{H}_m(k) &= H_m(k)w_m(k), \\ \widehat{\prod_m}(k) &= \prod_m(k)w_m(k). \end{aligned} \tag{6}$$

2.2. Channel Estimation Overview [2–5] . In this section, we first give a short overview of pilot-assisted CE with a TDM pilot, and then pilot-assisted CE with a FDM pilot is presented.

2.2.1. CE with TDM Pilot. In pilot-assisted CE with a TDM-pilot, the transmission block consists of a number of an $(N_c + N_g)$-sample size frames (i.e., the pilot signal is transmitted in the first $(m = 0)$ frame followed by $N_d - 1$ data frames) are illustrated in Figure 4(a).

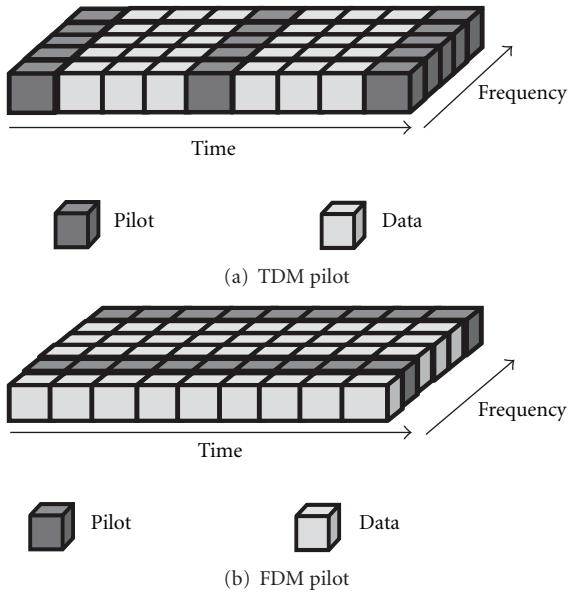

Figure 4: Pilot arrangements.

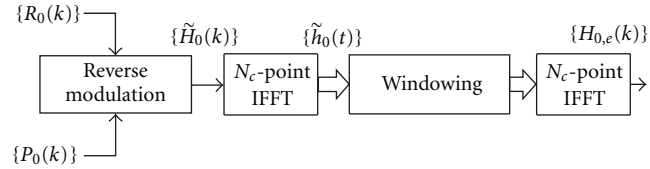

Figure 5: Block diagram for CE with TDM pilot.

Figure 5 illustrates the block diagram for a pilot-assisted CE with a TDM pilot. For $m = 0$, the instantaneous channel gain estimated at the kth frequency is obtained by reverse modulation as $\widetilde{H}_0(k) = R_0(k)/P(k)$ for $k = 0 \sim N_c - 1$, where $P(k)$ is the kth frequency component of the time-domain pilot signal $p(t)$. In this case, we use the Chu pilot sequence given by $\{p(t) = \exp(j\pi t^2/N_c);\ t = 0 \sim N_c - 1\}$ [20]. An N_c-point IFFT is performed on $\{\widetilde{H}_0(k);\ k = 0 \sim N_c - 1\}$ to obtain the instantaneous channel impulse response $\{\widetilde{h}_0(t);\ t = 0 \sim N_c - 1\}$. Assuming that the channel impulse response is present only within the GI, the estimated channel impulse response beyond the GI is replaced with zeros to reduce the noise [21], and an improved channel impulse response $\{\widehat{h}_0(t);\ t = 0 \sim N_c - 1\}$ is obtained. Then, the N_c-point FFT is applied to obtain the improved channel gain estimates $\{H_{0,e}(k);\ k = 0 \sim N_c - 1\}$ given by

$$\begin{aligned} H_{0,e}(k) &= \sum_{t=0}^{N_c-1} \widehat{h}_0(t) \exp\left(-j2\pi k \frac{t}{N_c}\right) \\ &= \sqrt{\frac{2E_s}{T_c N_c}}\left[H_0(k) + \frac{\Phi_0(k)}{P(k)}\right] + \frac{\prod_0(k)}{P(k)} \end{aligned} \tag{7}$$

for $k = 0 \sim N_c - 1$, where $\Phi_0(k)$ and $\prod_0(k)$, respectively, denote the distorted part of the channel gain estimates at the 0th frame due to the quantization and AWGN at the kth subcarrier.

2.2.2. CE with FDM Pilot. In pilot-assisted CE using the FDM pilot the frequency-domain interpolation is used over N_m equally-spaced pilot subcarriers as a subset of N_c subcarriers. In [22], it was shown that the optimum FDM-pilot scheme is the one with equally spaced inserted pilots. We also note here that the amplitude saturation level β has no effect on the optimal distribution of the pilot subcarriers, since the nonlinear noise is a random variable that is equally distributed over all the subcarriers in the frequency domain by the receiver's FFT.

The channel gain estimates $\{\widetilde{H}_m(q);\ q = \lfloor k/N_m \rfloor$ for $k = 0 \sim N_c - 1\}$ obtained by the reverse modulation can be expressed as

$$\begin{aligned} \widetilde{H}_m(q) &= \sqrt{\frac{2E_s}{T_c N_c}}[\alpha d_m(q) + \Lambda_m(q) + \Phi_m(q)]\frac{H_m(q)}{P(q)} \\ &\quad + \frac{\prod_m(q)}{P(q)}, \end{aligned} \tag{8}$$

where N_m represents the number of pilot subcarriers. Since $q = \lfloor k/N_m \rfloor$, the channel estimates are obtained only at the frequencies $k = 0, N_m, 2N_m, \ldots, N_c - 1$. Hence, an interpolation is required to obtain the channel gains for all frequencies (i.e., $k = 0 \sim N_c - 1$). First, the N_m-point IFFT is performed on $\{\widetilde{H}_m(q);\ q = 0 \sim N_m - 1\}$ to obtain the instantaneous channel impulse response $\{\widetilde{h}_m(t);\ t = 0 \sim N_m - 1\}$. $\{\widetilde{h}_m(t)\}$ is then fed to the N_c-point FFT to obtain the interpolated channel-gain estimates $\{H_{m,e}(k);\ k = 0 \sim N_c - 1\}$, which can be represented by

$$\begin{aligned} &H_{m,e}(k) \\ &\quad = \sum_{q=0}^{N_m-1} \widetilde{H}_m(q)\Psi(k,q) \\ &\quad = \sqrt{\frac{2E_s}{T_c N_c}}\left[H_m(k) + \sum_{q=0}^{N_m-1} \frac{\Lambda_m(k) + \Phi_m(k)}{P(k)}\Psi(k,q)\right] \\ &\qquad + \sum_{q=0}^{N_m-1} \frac{\prod_m(k)}{P(k)}\Psi(k,q), \end{aligned} \tag{9}$$

where

$$\begin{aligned} \Psi(k,q) &= \frac{\sin(\pi N_m(((N_m/N_c)q - k)/N_c))}{\sin(\pi(((N_m/N_c)q - k)/N_c))} \\ &\quad \times \exp(-j\pi(N_m - 1)(N_m/N_c)q - k/N_c), \end{aligned} \tag{10}$$

for $k = 0 \sim N_c - 1$. In (9), $\Lambda_m(k)$ and $\Phi_m(k)$, respectively, denote the mth frame's distorted part of the channel gain estimates due to the HPA saturation and quantization at the kth subcarrier.

3. Performance Analysis

In this section, first the closed-form BER expressions for pilot-assisted CE with both TDM and FDM pilots in a nonlinear and frequency-selective fading channel are presented, and then the estimator's MSE under the same conditions is evaluated.

To date, there have been a lot of papers based on computer simulation for both TDM and FDM pilots, but the theoretical analysis in a nonlinear and frequency-selective channel has not been presented. The probability density functions (PDFs) of the channel estimation error for both TDM and FDM pilot CE are evaluated with computer simulation in Figure 6. It is evident from Figure 6 that the standard deviation is higher for the FDM pilot, since the channel estimation error values are spread over a wider range. Since Chu sequence is used as TDM pilot with a constant (practicaly a very low) amplitudes in both the time and frequency domains, the channel estimator is only affected by pilot quantization giving the sharper shape on CE error's PDF in Figure 6. On the contrary, the shape of CE error's PDF for the FDM pilot is more spread, since the pilot subcarriers are affected by nonlinear noise due to both the HPA and the quantization. Naturally, this will have a negative effect on the FDM pilot performance in comparison with TDM pilot. This will be more discussed in details in Section 4.2.

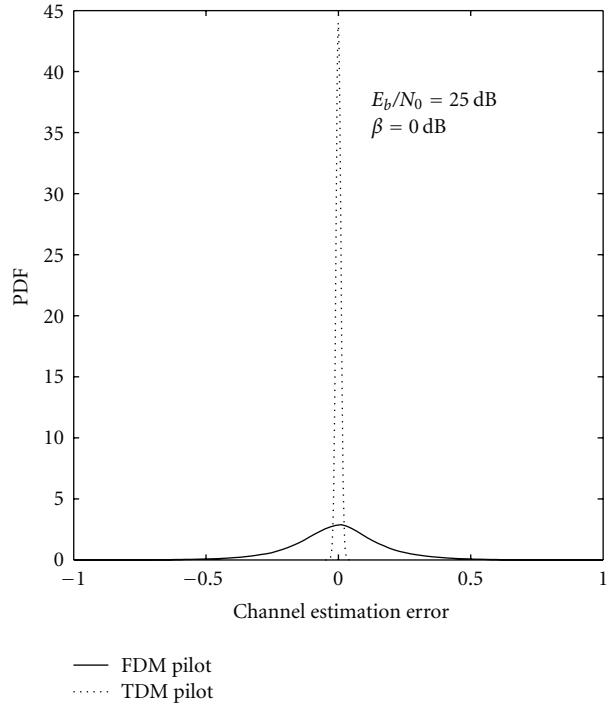

Figure 6: PDF of the estimator's error.

3.1. BER. We note here that in this analysis, only uniform quantization is considered, since in the case of nonuniform quantization, the quantization errors may not be approximated as Gaussian random variables, and the analysis may become very difficult if not impossible. Our analysis is based on the Gaussian approximation of the nonlinear noise, and the suitability of this approximation is confirmed by computer simulation as shown in Figure 7.

In the following, we assume the quadrature-phase shift keying (QPSK) for data modulation. The decision variables can be represented by $\hat{d}_m(k) = XY^*$ [1], where $X = R_m(k)$ and $Y = H_{m,e}(k)$ are assumed to be Gaussian random variables for $k = 0 \sim N_c - 1$. Thus, the BER for the mth frame is obtained as $P_{b,m} = \text{Prob}[\text{Re}(XY^*) < 0]$, while the average BER is obtained by [1]

$$P_b = \frac{1}{N_d - 1} \sum_{m=1}^{N_d - 1} \frac{1}{2} \left(1 - \frac{\text{Real}[\mu]}{\sqrt{1 - \text{Im}^2[\mu]}} \right), \tag{11}$$

where μ denotes the normalized covariance given by $\mu = m_{xy}/\sqrt{m_{xx} m_{yy}}$. Here, $m_{xx} = E[|X|^2]$, $m_{yy} = E[|Y|^2]$ and $m_{xy} = E[XY^*]$ denote the second moments of the random variables X, Y, and XY, respectively. Next, we derive the closed-form BER expression in a nonlinear and frequency-selective fading channel with both TDM and FDM pilots.

3.1.1. TDM Pilot. Using (4) and (7), the random variables $X$and Y are given by

$$\begin{aligned} X &= \sqrt{\frac{2E_s}{T_c N_c}} [\alpha d_m(k) + \Lambda_m(k) + \Phi_m(k)] H_m(k) + \prod_m (k), \\ Y &= \sqrt{\frac{2E_s}{T_c N_c}} \left[H_0(k) + \frac{\Phi_0(k)}{P(k)} \right] + \frac{\prod_0(k)}{P(k)}, \end{aligned} \tag{12}$$

where $\prod_0(k)$ denotes the AWGN at the kth frequency for $k = 0 \sim N_c - 1$. Using (12), the second moments m_{xx}, m_{yy}, and m_{xy} are given by the appendix

$$\begin{aligned} m_{xx} &= \frac{2E_s}{T_c N_c} \left[\alpha^2 + \frac{1}{N_c} (1 - \exp(-\beta^2) - \alpha^2) \right] \\ &\quad + \frac{2E_s}{T_c N_c} \frac{\Delta^2}{6} + \frac{2N_0}{T_c N_c}, \\ m_{yy} &= \frac{2E_s}{T_c N_c} (A_1 + A_2), \\ m_{xy} &= \frac{2E_s}{T_c N_c} A_3, \end{aligned} \tag{13}$$

with

$$\begin{aligned} A_1 &= 1 + \frac{\Delta^2}{6}, \\ A_2 &= \left(\frac{E_s}{N_0} \right)^{-1}, \\ A_3 &= \alpha J_0(2\pi f_D T_s \text{m}). \end{aligned} \tag{14}$$

The pilot-assisted CE using a TDM pilot has a problem with the propagation errors, since the estimated channel

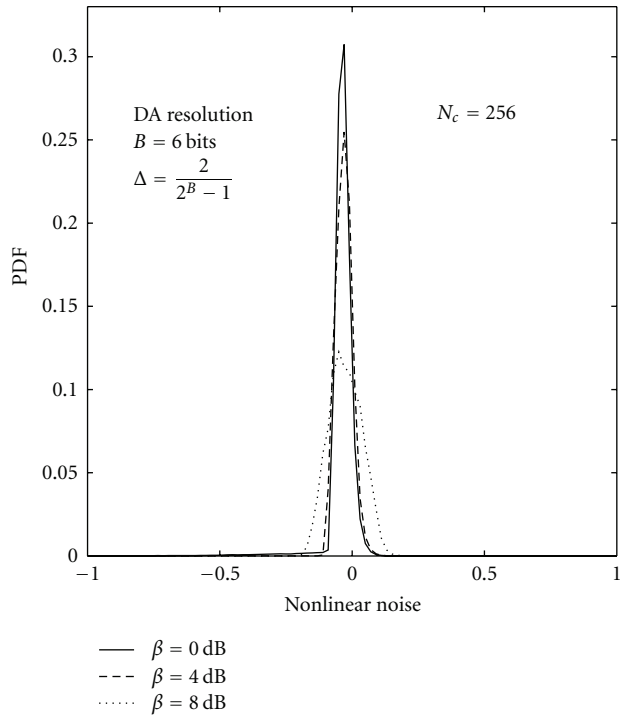

Figure 7: PDF of the nonlinear noise.

gains at the first and the channel gain at the last frame of the block vary due to channel time selectivity caused by the user mobility. We note here that the propagation error effect is captured in (13) by the coefficient A_3. After some manipulations, the normalized covariance μ^{TDM} for CE with the TDM pilot is given by

$$\mu^{\mathrm{TDM}} = \frac{A_3}{\sqrt{[\alpha^2 + B_1 + B_2][A_1 + A_2]}}, \tag{15}$$

where

$$B_1 = \frac{1}{N_c}\left(1 - \exp\left(-\beta^2\right) - \alpha^2\right) + \frac{\Delta^2}{6}, \qquad B_2 = \left(\frac{E_s}{N_0}\right)^{-1}. \tag{16}$$

Finally, the average BER is obtained by (11).

3.1.2. FDM Pilot. Using (4) and (9), the random variables X and Y are given by

$$X = \sqrt{\frac{2E_s}{T_cN_c}}[\alpha d_m(k) + \Lambda_m(k) + \Phi_m(k)]H_m(k) + \prod_m(k),$$

$$Y = \sqrt{\frac{2E_s}{T_cN_c}}\left[H_m(k) + \sum_{q=0}^{N_m-1}\frac{\Lambda_m(k) + \Phi_m(k)}{P(k)}\Psi(k,q)\right] + \sum_{q=0}^{N_m-1}\frac{\prod_m(k)}{P(k)}\Psi(k,q). \tag{17}$$

Then, using (17), the second moments m_{xx}, m_{yy}, and m_{xy} are given by the appendix

$$m_{xx} = \frac{2E_s}{T_cN_c}\alpha^2 + \frac{2E_s}{T_cN_c}\frac{1}{N_c}\left(1 - \exp\left(-\beta^2\right) - \alpha^2\right) + \frac{2E_s}{T_cN_c}\frac{\Delta^2}{6} + \frac{2N_0}{T_cN_c},$$

$$m_{yy} = \frac{2E_s}{T_cN_c} + \frac{2E_s}{T_cN_c}\frac{N_m}{N_c}\left(1 - \exp\left(-\beta^2\right) - \alpha^2\right) + \frac{2E_s}{T_cN_c}N_m\frac{\Delta^2}{6} + \frac{2N_0}{T_cN_c},$$

$$m_{xy} = \frac{2E_s}{T_cN_c}\alpha + \left[\frac{2E_s}{T_cN_c}\frac{1}{N_c}\left(1 - \exp\left(-\beta^2\right) - \alpha^2\right) + \frac{2E_s}{T_cN_c}\frac{\Delta^2}{6} + \frac{2N_0}{T_cN_c}\right]\sum_{q=0}^{N_m-1}\Psi(k,q). \tag{18}$$

Thus, the normalized covariance μ^{FDM} for CE with the FDM pilot is given by

$$\mu^{\mathrm{FDM}} = \frac{\alpha + N_m(B_1 + B_2)}{\sqrt{[\alpha^2 + B_1 + B_2][1 + N_m(B_1 + B_2)]}}, \tag{19}$$

where B_1 and B_2 are defined in Section 3.1.1. Finally, the average BER is obtained by (11). We note that in the case of CE with the FDM pilot $N_d \to \infty$.

3.1.3. Ideal CE. For the ideal CE, we have $H_{m,e}(k) = H_m(k)$, and consequently, using (4), the random variables X and Y are given by

$$X = \sqrt{\frac{2E_s}{T_cN_c}}[\alpha d_m(k) + \Lambda_m(k) + \Phi_m(k)]H_m(k) + \prod_m(k), \qquad Y = H_m(k). \tag{20}$$

Then, m_{xx}, m_{yy}, and m_{xy} are given by

$$m_{xx} = \frac{2E_s}{T_cN_c}\alpha^2 + \frac{2E_s}{T_cN_c}\frac{1}{N_c}\left(1 - \exp\left(-\beta^2\right) - \alpha^2\right) + \frac{2E_s}{T_cN_c}\frac{\Delta^2}{6} + \frac{2N_0}{T_cN_c},$$

$$m_{yy} = 1,$$

$$m_{xy} = \sqrt{\frac{2E_s}{T_cN_c}}\left[\alpha + \frac{1}{N_c}\left(1 - \exp\left(-\beta^2\right) - \alpha^2\right) + \frac{\Delta^2}{6}\right]. \tag{21}$$

Thus, we obtain the normalized covariance μ^{IDEAL} as

$$\mu^{\mathrm{IDEAL}} = \frac{\alpha + B_1 + B_2}{\sqrt{\alpha^2 + B_1 + B_2}}, \tag{22}$$

where B_1 and B_2 are defined in (15). Finally, the average BER is obtained by (11).

3.2. MSE. We define the MSE of the mth frame at the kth subcarrier as $\mathrm{MSE}_m(k) = E[|e_m(k)|^2] = E[|H_{m,e}(k) - H_m(k)|^2]$ and assume that the HPA amplitude saturation level β is known at the receiver.

3.2.1. TDM Pilot. For CE based on the TDM pilot, the nonlinearity effects the estimation process to a small extent. Thus, it can be neglected, since the Chu pilot sequence with a constant amplitude in both the time and frequency domains is used (i.e., the attenuation constant $\alpha = 1$). However, the quantization noise is present in (7), and consequently, for the TDM pilot we obtain

$$\mathrm{MSE}_{\mathrm{TDM}} = \frac{\Delta^2}{6} + \frac{1}{2}\left(1 + \frac{N_g}{N_c}\right)\left(\frac{E_b}{N_0}\right)^{-1}, \tag{23}$$

where $E_b/N_0 = 1/2(1 + N_g/N_c)(E_s/N_0)$. The first term in (23) denotes the negative effect of the nonlinearity due to the quantization, while the second term denotes the influence of AWGN.

3.2.2. FDM Pilot. CE with the FDM pilot requires a frequency interpolation. Thus, the nonlinear noise due to the quantization and HPA amplitude saturation is spread over data subcarriers after the interpolation. Using (9), we obtain the average MSE of the channel estimator with the FDM pilot given by

$$\begin{aligned}\mathrm{MSE}_{\mathrm{FDM}} = {} & \frac{N_m}{N_c}\left(1 - \exp(-\beta^2) - \alpha^2\right) + N_m\frac{\Delta^2}{6} \\ & + \frac{N_m}{2}\left(1 + \frac{N_g}{N_c}\right)\left(\frac{E_b}{N_0}\right)^{-1},\end{aligned} \tag{24}$$

where the first, the second, and the last term denote the negative effect of the nonlinearity due to the HPA amplitude saturation, quantization, and AWGN, respectively.

4. Numerical Results and Discussions

The OFDM-based system assumptions used in the computer simulation are given in Table 1. We assume an OFDM signal with $N_c = 256$ subcarriers, $N_g = 16$, $N_m = 16$, and QPSK data modulation. As the propagation channel, we assume an $L = 8$-path block Rayleigh fading channel with a uniform power-delay profile; $\{h_l;\ l = 0 \sim L - 1\}$ are independent and identically distributed zero-mean complex Gaussian variables having the variance 1/8. It is assumed that the time delay of the lth path is $\tau_l = l$ samples (i.e., the maximum delay difference is less than the GI length, since $L < N_g$). We have chosen $f_D T_s = 0.0001$ for the normalized Doppler frequency (where $1/T_s = 1/[T_c(1 + N_g/N_c)]$), which corresponds to a terminal speed of 40 km/h for a 2 GHz carrier frequencyand a transmission data rate of $1/T_s =$ 100 Msymbols/sec. We assume that the data rate is kept the same for both the TDM and FDM pilot schemes since an equal number of pilot subcarriers is transmitted within the transmission block (i.e., in total $N_c = N_m N_d$ pilots are transmitted over N_d frames) irrespective of CE scheme. In the case of CE with the TDM pilot, we use a Chu-sequence as a pilot given by $\{p(t) = \exp(j\pi t^2/N_c);\ t = 0 \sim N_c - 1\}$ [20]. We emphasize here that the case of $\beta \to \infty$ and $\Delta = 0$ represents a linear HPA and an ideal quantizer.

Table 1: Numerical parameters.

Transmitter	Data modulation	QPSK
	IFFT/FFT size	$N_c = 256$
	GI	$N_g = 16$
Channel	$L = 8$-path frequency-selective block Rayleigh fading	
Receiver	FDE	MRC
	Channel estimation	TDM and FDM pilots

4.1. BER. First, we evaluate the BER performance with pilot-assisted CE using both TDM and FDM pilots in a nonlinear and frequency-selective fading channel. The analytical and simulation results in terms of the average BER performance as a function of the E_b/N_0 with amplitude saturation level β as a parameter are illustrated in Figure 8(a) for $\Delta = 0$, that is, without considering the quantization noise. When we include the quantization noise ($\Delta = 0.05$), the BER performance is further degraded, as shown in Figure 8(b). However, the BER performance with CE using the FDM pilot becomes significantly worse. This is because with CE using a FDM pilot, the pilot subcarriers in addition to degradation due to quantization are affected by the HPA as well. Moreover, the frequency-domain interpolation will cause spreading of the nonlinear noise over all the subcarriers leading to a larger BER performance degradation in comparison with CE using the TDM pilot. However, the BER performance with pilot-assisted CE using the TDM pilot is degraded as well, since the nonlinear noise due to the quantization cannot be neglected. It is evident that fairly good agreement between the theoretical and simulated results is achieved, which confirms the validity of our theoretical analysis presented in this paper.

4.2. MSE. Next, we investigated the effect of nonlinearity on the channel estimator with both the TDM and FDM pilots by numerically evaluating its MSE. For the CE with the TDM pilot, we select $N_d = 16$, while $N_m = 16$ for the CE with the FDM pilot, and consequently, the same transmission data rate is maintained.

The MSE of the channel estimator is shown in Figure 9. First, we show the impact of the quantization step Δ in Figure 9(a). It is evident from the figure that the HPA amplitude saturation level β does not affect the MSE of the channelestimator for the CE using the TDM pilot. This

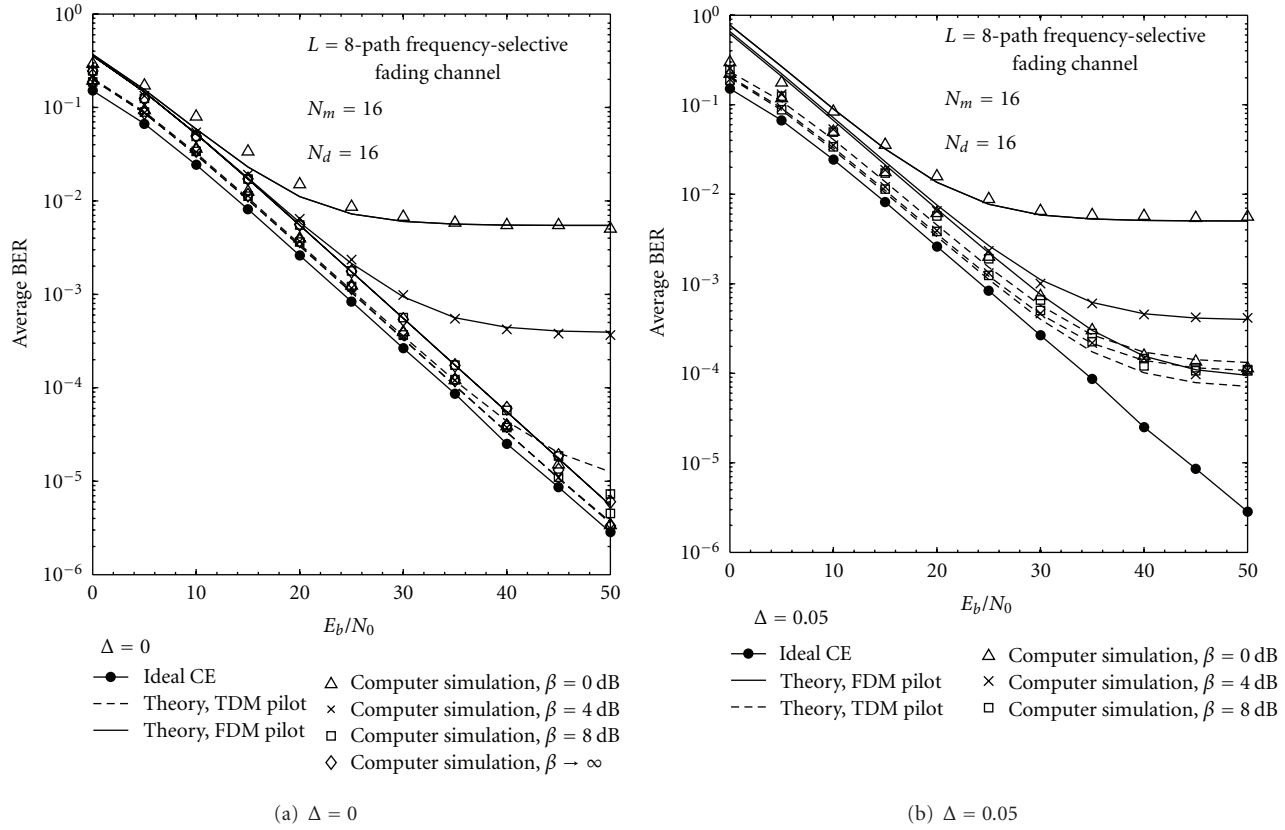

(a) Δ = 0 (b) Δ = 0.05

Figure 8: BER performance.

is because the performance is not affected by the HPA amplitude saturation for the CE using the TDM pilot, since we are using the Chu pilot sequence which has a constant amplitude in both the time and frequency domains.

The impact of the HPA amplitude saturation level β is presented in Figure 9(b) for value $E_b/N_0 = 35$ dB in order to better observe the effect of parameter Δ. It is evident that the quantization noise represented through quantization step Δ affects more the MSE of the channel estimator for the FDM-based pilot-assisted CE. Finally, in Figure 9(c), the impact of E_b/N_0 is plotted. In comparison with pilot-assisted CE with the TDM pilot, the MSE of the channel estimator with the pilot-assisted CE based on the FDM pilot is more affected by nonlinear noise. This is because for the CE with the TDM pilot the Chu pilot sequence is used with a constant (practically a very low) amplitudes in both the time and frequency domains, and consequently, the channel estimator's performance using the TDM pilot is not affected by the HPA. The nonlinear degradations in this case are only due to the quantization. This is because of the fact that for pilot-assisted CE using the FDM pilot, the pilot signals are inserted onto dedicated (i.e., pilot) subcarriers in frequency domain within the OFDM signal. Consequently, the corresponding OFDM signal in the time domain may have a large PAPR causing a signal degradation due to nonlinear noise coming from both the HPA and quantization. After the FFT at the receiver, the nonlinear noise will spread over all the subcarriers and affect the pilot subcarriers. Naturally, this will have a negative effect on the channel estimator's performance in comparison with the pilot-assisted CE using the TDM pilot.

5. Conclusions

In this paper, we have presented closed-form BER expressions for OFDM with CE based on both TDM and FDM pilots in a nonlinear and frequency-selective fading channel. In our analysis the nonlinear noise is approximated with a Gaussian random variable, where unlike previous studies, we consider the impact of both the DA converter and the HPA. The results show that the pilot-assisted CE with the FDM pilot is affected by the nonlinear noise due to both the quantization and the HPA, while the pilot-assisted CE with the TDM pilot is only affected by nonlinear degradation due to quantization because of the pilot-sequence with low PAPR. Thus, the higher BER with FDM pilot in comparison with TDM pilot is observed. Furthermore, numerical results have confirmed the validity of the analytical derivations in terms of closed-form BER expressions, since a fairly good agreement between the simulation and the analytical results is observed.

Appendix

Here, we present a derivation of the second moments of the random variables X and Y given by m_{xx}, m_{yy}, and m_{xy}.

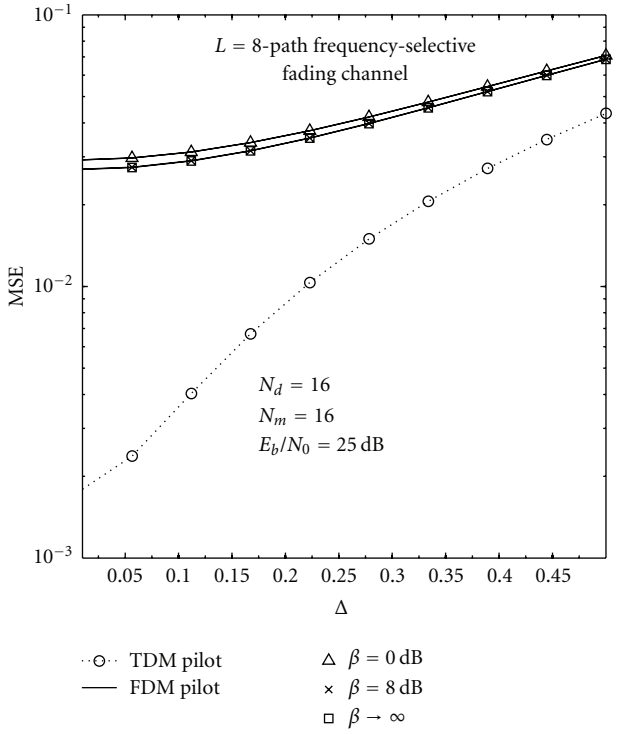

(a) Impact of Δ

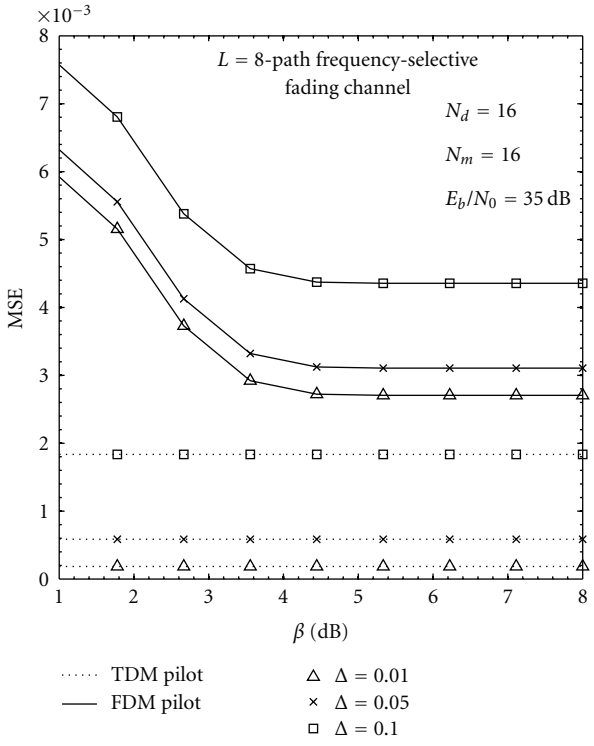

(b) Impact of β

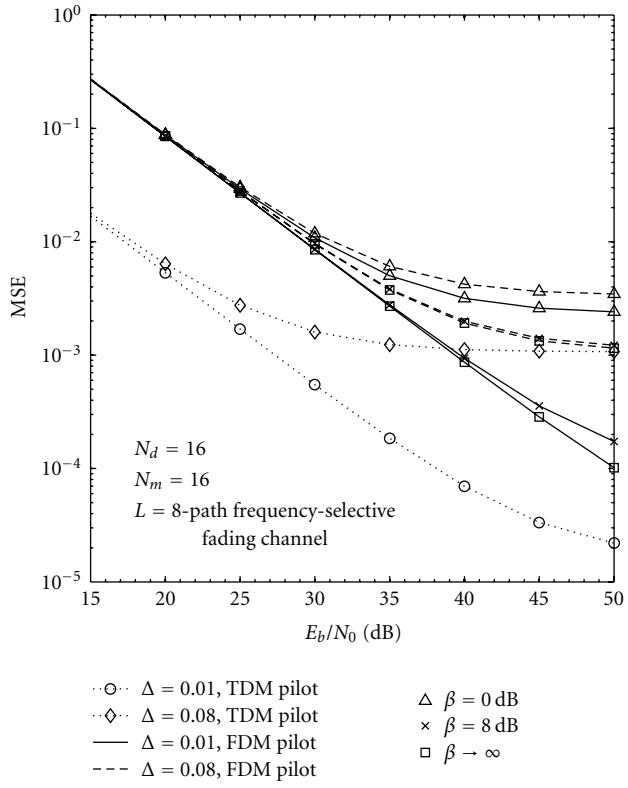

(c) Impact of E_b/N_0

Figure 9: MSE of the channel estimator.

(1) *TDM pilot.* Using (4) the second moment m_{xx} of the random variable X is given by

$$\begin{aligned}
m_{xx} &= E\Bigg[\left(\sqrt{\frac{2E_s}{T_cN_c}}\alpha d_m(k)H_m(k)+\sqrt{\frac{2E_s}{T_cN_c}}\Lambda_m(k)H_m(k)\right.\\
&\qquad\left.+\sqrt{\frac{2E_s}{T_cN_c}}\Phi_m(k)H_m(k)+\prod_m(k)\right)\\
&\qquad\times\left(\sqrt{\frac{2E_s}{T_cN_c}}\alpha d_m(k)H_m(k)+\sqrt{\frac{2E_s}{T_cN_c}}\Lambda_m(k)H_m(k)\right.\\
&\qquad\left.+\sqrt{\frac{2E_s}{T_cN_c}}\Phi_m(k)H_m(k)+\prod_m(k)\right)^*\Bigg]\\
&= \frac{2E_s}{T_cN_c}\alpha^2E\left[|d_m(k)|^2\right]+\frac{2E_s}{T_cN_c}E\left[|\Lambda_m(k)|^2\right]E\left[|H_m(k)|^2\right]\\
&\quad+\frac{2E_s}{T_cN_c}E\left[|\Phi_m(k)|^2\right]E\left[|H_m(k)|^2\right]+E\left[\left|\prod_m(k)\right|^2\right].
\end{aligned}\tag{A.1}$$

We assume that $E[|d_m(k)|^2]=1$ with $E[|H_m(k)|^2]=1$, and after the expectation over the noise terms the, second moment m_{xx} of the random variable X is obtained as

$$m_{xx}=\frac{2E_s}{T_cN_c}\left[\alpha^2+\frac{1}{N_c}\left(1-\exp\left(-\beta^2\right)-\alpha^2\right)+\frac{\Delta^2}{6}\right]+\frac{2N_0}{T_cN_c}.\tag{A.2}$$

Using (7), the second moment m_{yy} of the random variable Y is given by

$$\begin{aligned}
m_{yy} &= E\Bigg[\left(\sqrt{\frac{2E_s}{T_cN_c}}H_0(k)+\sqrt{\frac{2E_s}{T_cN_c}}\frac{\Phi_m(k)}{P(k)}+\frac{\prod_0(k)}{P(k)}\right)\\
&\qquad\times\left(\sqrt{\frac{2E_s}{T_cN_c}}H_0(k)+\sqrt{\frac{2E_s}{T_cN_c}}\frac{\Phi_m(k)}{P(k)}+\frac{\prod_0(k)}{P(k)}\right)^*\Bigg]\\
&= \frac{2E_s}{T_cN_c}+\frac{2E_s}{T_cN_c}\frac{E\left[|\Phi_m(k)|^2\right]}{E\left[|P(k)|^2\right]}+\frac{E\left[|\prod_0(k)|^2\right]}{E\left[|P(k)|^2\right]}.
\end{aligned}\tag{A.3}$$

We assume Chu pilot sequence with $E[|P(k)|^2]=1$, and after the expectation over the noise terms, the second moment m_{yy} of the random variable Y is obtained as

$$m_{yy}=\frac{2E_s}{T_cN_c}\left[1+\frac{\Delta^2}{6}+\frac{N_0}{E_s}\right].\tag{A.4}$$

Finally, the second moment m_{xy} of the random variables X and Y is given by

$$\begin{aligned}
m_{xy} &= E\Bigg[\left(\sqrt{\frac{2E_s}{T_cN_c}}\alpha d_m(k)H_m(k)+\sqrt{\frac{2E_s}{T_cN_c}}\Lambda_m(k)H_m(k)\right.\\
&\qquad\left.+\sqrt{\frac{2E_s}{T_cN_c}}\Phi_m(k)H_m(k)+\prod_m(k)\right)\\
&\qquad\times\left(\sqrt{\frac{2E_s}{T_cN_c}}H_0(k)+\sqrt{\frac{2E_s}{T_cN_c}}\frac{\Phi_0(k)}{P(k)}+\frac{\prod_0(k)}{P(k)}\right)^*\Bigg]\\
&= \frac{2E_s}{T_cN_c}\alpha E\left[H_m(k)H_0^*(k)\right]+\frac{2E_s}{T_cN_c}E\left[\Phi_m(k)\Phi_0^*(k)\right]\\
&\quad+E\left[\prod_m(k)\prod_0^*(k)\right].
\end{aligned}\tag{A.5}$$

Due to the fact that the nonlinear noise and the AWGN component at the 0th and mth frames are uncorrelated (i.e., $E[\Phi_m(k)\Phi_0^*(k)]=0$ and $E[\prod_m(k)\prod_0^*(k)]=0$), and the Jakes fading model assumption, the second moment m_{xy} of the random variables X and Y is obtained as

$$m_{xy}=\frac{2E_s}{T_cN_c}\alpha J_0\left(2\pi f_DT_sm\right).\tag{A.6}$$

(2) *FDM pilot.* Using (4) the second moment m_{xx} of the random variable X is given by

$$\begin{aligned}
m_{xx} &= E\Bigg[\left(\sqrt{\frac{2E_s}{T_cN_c}}\alpha d_m(k)H_m(k)+\sqrt{\frac{2E_s}{T_cN_c}}\Lambda_m(k)H_m(k)\right.\\
&\qquad\left.+\sqrt{\frac{2E_s}{T_cN_c}}\Phi_m(k)H_m(k)+\prod_m(k)\right)\\
&\qquad\times\left(\sqrt{\frac{2E_s}{T_cN_c}}\alpha d_m(k)H_m(k)+\sqrt{\frac{2E_s}{T_cN_c}}\Lambda_m(k)H_m(k)\right.\\
&\qquad\left.+\sqrt{\frac{2E_s}{T_cN_c}}\Phi_m(k)H_m(k)+\prod_m(k)\right)^*\Bigg]\\
&= \frac{2E_s}{T_cN_c}\alpha^2+\frac{2E_s}{T_cN_c}E\left[|\Lambda_m(k)|^2\right]+\frac{2E_s}{T_cN_c}E\left[|\Phi_m(k)|^2\right]\\
&\quad+E\left[\left|\prod_m(k)\right|^2\right],
\end{aligned}\tag{A.7}$$

and after the expectation over the noise terms, the second moment m_{xx} of the random variable X is obtained as

$$m_{xx}=\frac{2E_s}{T_cN_c}\left[\alpha^2+\frac{1}{N_c}\left(1-\exp\left(-\beta^2\right)-\alpha^2\right)+\frac{\Delta^2}{6}\right]+\frac{2N_0}{T_cN_c}.\tag{A.8}$$

Using (9), the second moment m_{yy} of the random variable Y is given by

$$
\begin{aligned}
m_{yy} &= E\Bigg[\Bigg(\sqrt{\frac{2E_s}{T_cN_c}}H_m(k)+\sqrt{\frac{2E_s}{T_cN_c}}\sum_{q=0}^{N_m-1}\frac{\Lambda_m(k)}{P(k)}\Psi(k,q)\\
&\quad+\sqrt{\frac{2E_s}{T_cN_c}}\sum_{q=0}^{N_m-1}\frac{\Phi_m(k)}{P(k)}\Psi(k,q)+\sum_{q=0}^{N_m-1}\frac{\prod_m(k)}{P(k)}\times\Psi(k,q)\Bigg)\\
&\quad\times\Bigg(\sqrt{\frac{2E_s}{T_cN_c}}H_m(k)+\sqrt{\frac{2E_s}{T_cN_c}}\sum_{q=0}^{N_m-1}\frac{\Lambda_m(k)}{P(k)}\Psi(k,q)\\
&\quad+\sqrt{\frac{2E_s}{T_cN_c}}\sum_{q=0}^{N_m-1}\frac{\Phi_m(k)}{P(k)}\Psi(k,q)\\
&\quad+\sum_{q=0}^{N_m-1}\frac{\prod_m(k)}{P(k)}\times\Psi(k,q)\Bigg)^*\Bigg]\\
&=\frac{2E_s}{T_cN_c}+\frac{2E_s}{T_cN_c}\frac{E\left[|\Phi_m(k)|^2\right]}{E\left[|P(k)|^2\right]}N_m+\frac{2E_s}{T_cN_c}\frac{E\left[|\Lambda_m(k)|^2\right]}{E\left[|P(k)|^2\right]}N_m\\
&\quad+\frac{E\left[|\prod_m(k)|^2\right]}{E\left[|P(k)|^2\right]}.
\end{aligned}
\tag{A.9}
$$

We assume that $E[|P(k)|^2]=1$ for FDM pilot, and after the expectation over the noise terms, the second moment m_{yy} of the random variable Y is obtained as

$$
m_{yy}=\frac{2E_s}{T_cN_c}\left[1+\frac{N_m}{N_c}(1-\exp(-\beta^2)-\alpha^2)+N_m\frac{\Delta^2}{6}\right]+\frac{2N_0}{T_cN_c}.
\tag{A.10}
$$

Finally, the second moment m_{xy} of the random variables X and Y is given by

$$
\begin{aligned}
m_{xy} &= E\Bigg[\Bigg(\sqrt{\frac{2E_s}{T_cN_c}}\alpha d_m(k)H_m(k)+\sqrt{\frac{2E_s}{T_cN_c}}\Lambda_m(k)H_m(k)\\
&\quad+\sqrt{\frac{2E_s}{T_cN_c}}\Phi_m(k)H_m(k)+\prod_m(k)\Bigg)\\
&\quad\times\Bigg(\sqrt{\frac{2E_s}{T_cN_c}}H_m(k)+\sqrt{\frac{2E_s}{T_cN_c}}\sum_{q=0}^{N_m-1}\frac{\Lambda_m(k)+\Phi_m(k)}{P(k)}\\
&\quad\times\Psi(k,q)+\sum_{q=0}^{N_m-1}\frac{\prod_m(k)}{P(k)}\Psi(k,q)\Bigg)^*\Bigg]\\
&=\frac{2E_s}{T_cN_c}\alpha+\frac{2E_s}{T_cN_c}E\left[|\Lambda_m(k)|^2\right]\sum_{q=0}^{N_m-1}\Psi(k,q)\\
&\quad+\frac{2E_s}{T_cN_c}E\left[|\Phi_m(k)|^2\right]\sum_{q=0}^{N_m-1}\Psi(k,q)\\
&\quad+E\left[\left|\prod_m(k)\right|^2\right]\sum_{q=0}^{N_m-1}\Psi(k,q).
\end{aligned}
\tag{A.11}
$$

After performing expectation over the noise terms, the second moment m_{xy} of the random variables X and Y is obtained as

$$
\begin{aligned}
m_{xy} &= \frac{2E_s}{T_cN_c}\alpha+\Bigg[\frac{2E_s}{T_cN_c}\frac{1}{N_c}(1-\exp(-\beta^2)-\alpha^2)+\frac{2E_s}{T_cN_c}\frac{\Delta^2}{6}\\
&\quad+\frac{2N_0}{T_cN_c}\Bigg]\sum_{q=0}^{N_m-1}\Psi(k,q).
\end{aligned}
\tag{A.12}
$$

Acknowledgment

This work was supported in part by Ministry of Civil Affairs of Bosnia and Herzegovina with support grant for preparation of EU FP7-related research projects.

References

[1] J. G. Proakis, *Digital Communications*, McGraw-Hill, New York, NY, USA, 3rd edition, 1995.

[2] S. Coleri, M. Ergen, A. Puri, and A. Bahai, "Channel estimation techniques based on pilot arrangement in OFDM systems," *IEEE Transactions on Broadcasting*, vol. 48, no. 3, pp. 223–229, 2002.

[3] M. H. Hsieh and C. H. Wei, "Channel estimation for OFDM systems based on comb-type pilot arrangement in frequency selective fading channels," *IEEE Transactions on Consumer Electronics*, vol. 44, no. 1, pp. 217–225, 1998.

[4] W. Zhang, X. G. Xia, and P. C. Ching, "Optimal training and pilot pattern design for OFDM systems in Rayleigh fading," *IEEE Transactions on Broadcasting*, vol. 52, no. 4, pp. 505–514, 2006.

[5] Y. S. Choi, P. J. Voltz, and F. A. Cassara, "On channel estimation and detection for multicarrier signals in fast and selective Rayleigh fading channels," *IEEE Transactions on Communications*, vol. 49, no. 8, pp. 1375–1387, 2001.

[6] H. Schmidt and K.-D. Kammeyer, "Quantization and its effects on OFDM concepts for wireless indoor applications," in *Proceedings of the 4th International OFDM-Workshop (InOWo '99)*, Hamburg, Germany, 1999.

[7] S. Xiaoying and C. H. Slump, "Quantization effects in OFDM system," in *Proceedings of the 29th Symposium on Information Theory in the Benelux*, pp. 93–103, Leuven, Belgium, May 2008.

[8] D. Dardari, "Joint clip and quantization effects characterization in OFDM receivers," *IEEE Transactions on Circuits and Systems I*, vol. 53, no. 8, pp. 1741–1748, 2006.

[9] H. Yang, T. C. W. Schenk, P. F. M. Smulders, and E. R. Fledderus, "Joint impact of quantization and clipping on single- and multi-carrier block transmission systems," in *Proceedings of the IEEE Wireless Communications and Networking*

Conference (WCNC '08), pp. 548–553, Las Vegas, Nev, USA, 2008.

[10] M. Sawada, H. Okada, T. Yamazato, and M. Katayama, "Influence of ADC nonlinearity on the performance of an OFDM receiver," *IEICE Transactions on Communications*, vol. 89, no. 12, pp. 3250–3256, 2006.

[11] T. Araujo and R. Dinis, "Performance evaluation of quantization effects on multicarrier modulated signals," *IEEE Transactions on Vehicular Technology*, vol. 56, no. 5, pp. 2922–2930, 2007.

[12] T. Araujo and R. Dinis, "Analytical evaluation of nonlinear effects on OFDMA signals," *IEEE Transactions on Wireless Communications*, vol. 9, no. 11, pp. 3472–3479, 2010.

[13] H. G. Ryu, T. P. Hoa, N. T. Hieu, and J. Jianxue, "BER analysis of clipping process in the forward link of the OFDM-FDMA communication system," *IEEE Transactions on Consumer Electronics*, vol. 50, no. 4, pp. 1058–1064, 2004.

[14] G. P. White, A. G. Burr, and T. Javornik, "Modelling of nonlinear distortion in broadband fixed wireless access systems," *Electronics Letters*, vol. 39, no. 8, pp. 686–687, 2003.

[15] X. Li and L. J. Cimini, "Effects of clipping and filtering on the performance of OFDM," *IEEE Communications Letters*, vol. 2, no. 5, pp. 131–133, 1998.

[16] A. Papoulis, *Probability, Random Variables, and Stochastic Processes*, McGraw-Hill, New York, NY, USA, 3rd edition, 1991.

[17] D. Dardari, V. Tralli, and A. Vaccari, "A theoretical characterization of nonlinear distortion effects in ofdm systems," *IEEE Transactions on Communications*, vol. 48, no. 10, pp. 1755–1764, 2000.

[18] P. Banelli and S. Cacopardi, "Theoretical analysis and performance of OFDM signals in nonlinear AWGN channels," *IEEE Transactions on Communications*, vol. 48, no. 3, pp. 430–441, 2000.

[19] S. Hara and R. Prasad, "Overview of multicarrier CDMA," *IEEE Communications Magazine*, vol. 35, no. 12, pp. 126–144, 1997.

[20] D. C. Chu, "Polyphase codes with good periodic correlation properties," *IEEE Transactions on Information Theory*, vol. 18, no. 4, pp. 531–532, 1972.

[21] O. Edfors, M. Sandell, J. J. D. Van Beek, S. K. Wilson, and P. O. Borjesson, "OFDM channel estimation by singular value decomposition," *IEEE Transactions on Communications*, vol. 46, no. 7, pp. 931–939, 1998.

[22] R. Negi and J. Cioffi, "Pilot tone selection for channel estimation in a mobile ofdm system," *IEEE Transactions on Consumer Electronics*, vol. 44, no. 3, pp. 1122–1128, 1998.